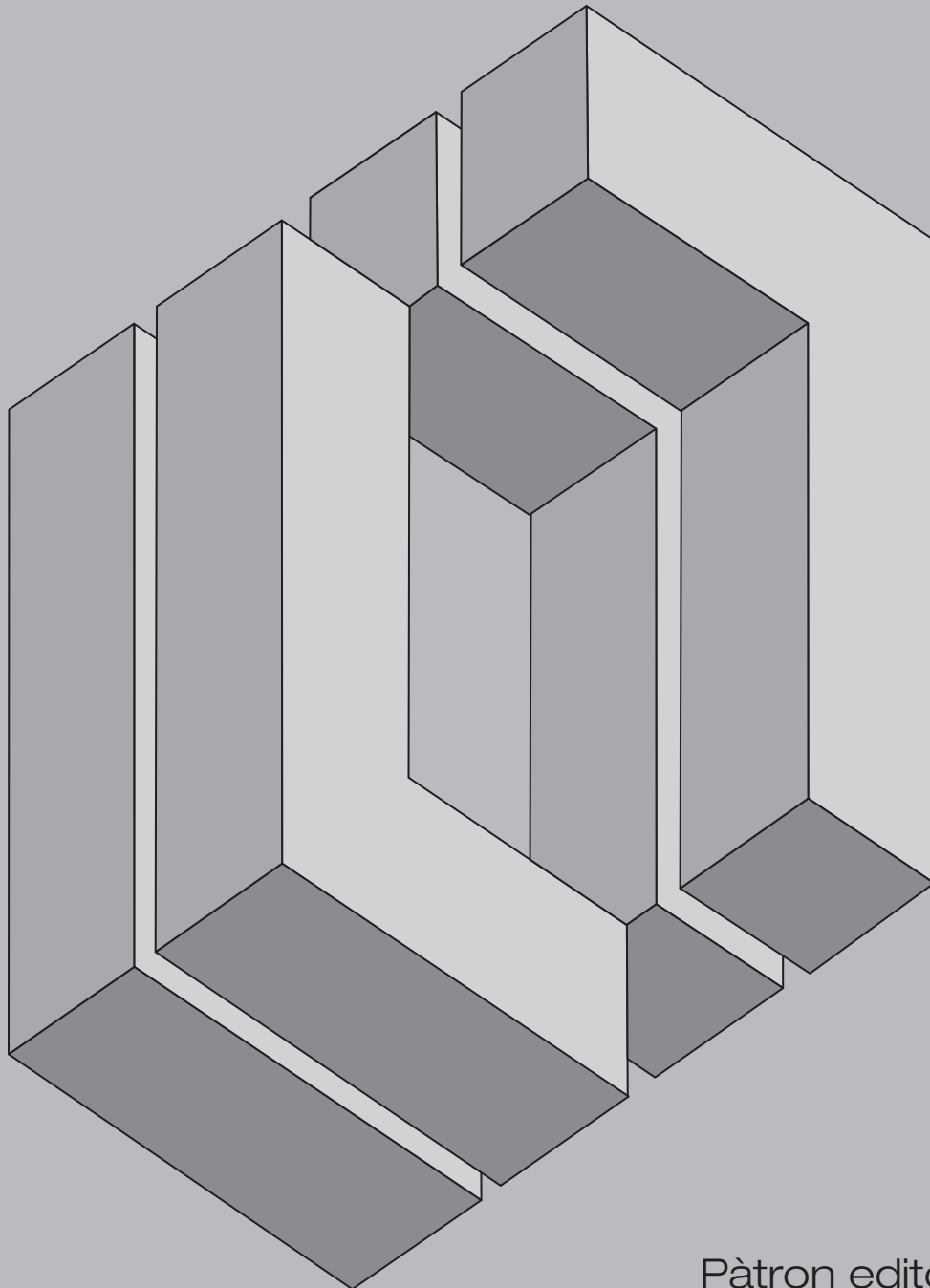
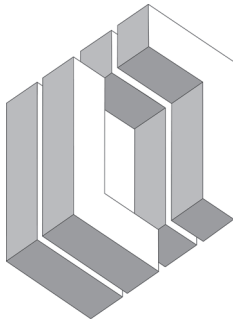


# *ingegneria sismica*

International Journal of Earthquake Engineering  
Trimestrale tecnico-scientifico

[www.ingegneriasismica.org](http://www.ingegneriasismica.org)





**Founder / Fondatore**

Duilio Benedetti – Politecnico di Milano

**Editor-in-Chief / Coordinatore editoriale**

Gianmario Benzoni – University of California San Diego – benzoni@ucsd.edu

**Associate Editors / Coordinatori associati**

Panayotis Caridys – National Technical University Athens, Greece  
Dina D'Ayala – University of Bath, UK  
Maria Adelaide Parisi – Politecnico di Milano, Italy

**Scientific Board / Comitato scientifico**

Raimondo Betti – Columbia University, USA  
Alfredo Campos Costa – LNEC Lisbon, Portugal  
Giacomo Di Pasquale – Dipartimento della Protezione Civile, Italy  
Giancarlo Gioda – Politecnico di Milano, Italy  
James M. Kelly – University of California Berkeley, USA  
Sergio Lagomarsino – Università di Genova, Italy  
Giuseppe Lomiento – Bianchi-Lomiento, Italy  
Claudia Madiai – Università degli Studi di Firenze, Italy  
Alessandro Martelli – ENEA Bologna, Italy  
Mauro Mezzina – Politecnico di Bari, Italy  
Maria Ofelia Moroni – Universidad de Chile, Santiago, Chile  
Stefano Pampanin – University of Canterbury, New Zealand  
Florian Pergalani – Politecnico di Milano, Italy  
Yuri Ribakov – Ariel University, Israel  
Paolo Rugarli – Castalia S.r.l. Milano, Italy  
Gaetano Russo – Università di Udine, Italy  
Milutin Srbulov – Mott McDonald, U.K.  
Miha Tomasevic – Slovenian Civil Engineering Institute, Slovenia  
Mihailo Trifunac – University of Southern California, USA  
Keh-Chyuan Tsai – National Taiwan University, Taipei, Taiwan  
Thomas Wenk – Swiss Society for Earthquake Eng., Switzerland  
Aspasia Zerva – Drexel University, USA

**Director / Direttore responsabile**

Fausto Giovannardi – Giovannardi e Rontini, Borgo San Lorenzo (FI), Italy

**Redazione, amministrazione, abbonamenti e pubblicità**

Patron Editore  
Via Badini 12, Quarto Inferiore  
40057 Granarolo dell'Emilia, Bologna  
Tel. (051) 767003 – Fax (051) 768252  
e-mail: info@patroneditore.com  
Sito: www.patroneditore.com

**Stampa:** Rabbi S.r.l. Bologna per conto della Patron editore  
Bologna, giugno 2015

**Subscriptions see URL:**  
[www.ingegneriasismica.org](http://www.ingegneriasismica.org)

**Abbonamenti 2014**  
€ 78,00; (estero € 110,00).  
**Fascicoli arretrati:**  
€ 21,00; (estero € 32,00).  
**Abbonamento cartaceo + on-line € 90,10 (estero € 135,41).**  
**Abbonamento on-line € 38,00.**  
**Abbonamento on-line + archivi € 60,50.**  
**Modalità di pagamento:**

PDF singoli articoli: [www.ingegneriasismica.org](http://www.ingegneriasismica.org)  
€ 15,00 se relativi all'anno in corso, € 6,50 precedenti all'anno in corso  
L'abbonamento ha decorrenza gennaio-dicembre, con diritto di ricevimento dei fascicoli già pubblicati, se sottoscritto in corso d'anno. I fascicoli non pervenuti possono essere richiesti non oltre 30 giorni dopo la spedizione del numero successivo.  
Inviare il versamento anticipato adottando una delle seguenti forme:  
– c.c.p. n.000016141400 intestato a Patron editore, via Badini 12, Quarto Inferiore, 40057 Granarolo dell'Emilia (BO)  
– bonifico bancario a CARISBO, Agenzia 68, Via Pertini 8, Quarto Inferiore, 40057, Granarolo dell'Emilia (BO) BIC IBSPIT2B; IBAN, IT 03 M 06385 36850 07400000782T  
– carta di credito a mezzo PAYPAL [www.paypal.it](http://www.paypal.it)

Sul sito [www.ingegneriasismica.org](http://www.ingegneriasismica.org) nella sessione archivi sono presenti tutti gli indici delle annate pubblicate.

Ingegneria Sismica  
Registrazione Tribunale di Bologna n. 5139 del 20.2.84  
Realizzazione grafica della copertina: Arturo Galletti

ASSOCIATO ALL'USPI  
UNIONE STAMPA  
PERIODICA ITALIANA



# ingegneria sismica

International Journal of Earthquake Engineering

Anno XXXI – N. 3-4 – luglio-dicembre 2014 – Pagine 112

**Sommario/Contents**

Preface	
M.P. LIMONGELLI	Pag. 3
On the Estimation of the Fundamental Modal Properties of Italian Historical Masonry Towers	
<i>Sulla stima delle proprietà dinamiche fondamentali delle torri storiche in muratura italiane</i>	
C. RAINIERI, A. MARRA, G. FABBROCINO	” 4
Damage Localization in a High-Rise Building Using Seismic Excitation	
<i>Localizzazione del danno in un edificio soggetto ad eccitazione sismica</i>	
M.P. LIMONGELLI, L. MARTINELLI, A. ZAMBRANO	” 17
Framed Structures: Detection of Building Torsional Modes Using a Simplified Experimental Approach	
<i>Un approccio semplificato per l'identificazione sperimentale dei modi rotazionali delle strutture intelaiate</i>	
R. DITOMMASO, M. VONA, A. MASI, M. MUCCIARELLI, F.C. PONZO	” 35
Dynamic and Seismic Health Monitoring of a Historic Masonry Tower	
<i>Monitoraggio dinamico e sismico di una torre storica in muratura</i>	
A. SAISI, C. GENTILE, M. GUIDOBALDI	” 45
Numerical and Experimental Assessment of the Performance of Four Nondestructive Damage Evaluation Methods in Situations Comparable to Post-Earthquake Damage Analysis	
<i>Valutazione numerica e sperimentale delle prestazioni di quattro metodi non distruttivi di identificazione del danno in situazioni analoghe ad analisi di danno post-terremoto</i>	
P. GUÉGUEN, A. HAMZE, L. BAILLET, P. ROUX	” 59
An Evaluation of a Methodology for Detection, Localization, and Quantification of Changes in Nonlinear Systems Based on Experimental Measurements	
<i>Valutazione di un metodo di identificazione, localizzazione e quantificazione di variazioni in sistemi non lineari sulla base di misure sperimentali</i>	
M.R. HERNANDEZ-GARCIA, S.F. MASRI, R. GHANEM, E. FIGUEIREDO, C.R. FARRAR	” 72
Localization of Damage Occurred on Framed Structures: Analysis of the Geometric Characteristics of the Fundamental Mode Shape	
<i>Localizzazione del danno sulle strutture intelaiate: analisi delle caratteristiche geometriche riferite alla deformata modale fondamentale</i>	
F.C. PONZO, R. DITOMMASO, G. AULETTA, C. IACOVINO, A. MOS-SUCCA, A. NIGRO, D. NIGRO	” 87
Numerical and Experimental Validation of a Structural Health Monitoring Technique for Critical Infrastructure	
<i>Validazione numerica e sperimentale di una tecnica di monitoraggio strutturale per infrastrutture</i>	
G. BENZONI, N. BONESSIO, G. LOMIENTO	” 102

**TO READERS AND AUTHORS**

We are pleased to announce that *Ingegneria Sismica* is covered by Compendex, one of Elsevier products. Compendex will index papers and possibly extract data from the full text. Coverage increases dissemination of authors' work: the benefits are high visibility to a global audience. Since 1970, Compendex has been the engineering database of choice for researchers, students, faculty and engineering professionals around the world.

**AI LETTORI ED AGLI AUTORI**

Siamo lieti di comunicare che *Ingegneria Sismica* fa parte del database di Compendex, uno dei prodotti di Elsevier. Questo comporta l'indicizzazione degli articoli pubblicati e la eventuale citazione di dati estratti dal testo. Verrà così fortemente accresciuta la visibilità internazionale degli autori e degli argomenti trattati. Compendex costituisce, fin dal 1970 un importante database per ricercatori, operatori accademici, studenti e professionisti di tutto il mondo.

# Numerical and Experimental Validation of a Structural Health Monitoring Technique for Critical Infrastructure

Gianmario Benzoni\*, Noemi Bonessio\*, Giuseppe Lomiento\*\*

**SUMMARY** – A Damage Identification method developed for infrastructure equipped with seismic response modification devices is hereafter summarized and validated through numerical and experimental case studies. The output-only method was tested via Finite Element analyses of two bridge structures, the Vincent Thomas Bridge and the Benicia Martinez Bridge, equipped with viscous dampers and friction pendulum bearings, respectively. The application of the method to real ambient vibration data from the Vincent Thomas Bridge proved successful in identifying early stages of degradation of seismic response modification devices. The Level III damage detection method was also applied to a three-span cable-stayed bridge, the Yokohama Bay Bridge, based on accelerometric records from the 2011 East Japan Earthquake. The integration of the method in an innovative monitoring systems aimed at the real-time remote assessment of the structural adequacy of aging critical infrastructure is under development.

**Keywords:** Structural health monitoring, Multi-mode damage identification, Sensor network, Critical infrastructure, Seismic isolators, Dampers.

## 1. Introduction

Since the early 1980s, great efforts have been dedicated to enhance the damage detection capability of vibration based SHM systems, as extensively described in (Carden et al, 2000). A number of monitoring programs for bridge structures all over the world are currently providing invaluable data broadly used for development and validation of a variety of structural identification methods (Lus et al., 1999, Smyth et al., 2003, Siringoringo et al., 2006, Yun et al., 2008, Soyoz et al., 2009) and of damage detection algorithms. The use of SHM for maintenance purposes are described in several recent papers for civil infrastructures (Aktan et al., 2000; Frangopol and Liu, 2007; Okasha and Frangopol, 2012).

When dealing with critical infrastructure such as long span cable-stayed and suspension bridges, geometric nonlinearities may affect significantly the dynamic structural behavior under intense excitations, while playing a limited role in low amplitude ambient-vibrations. Even if nonlinear reduced-order models appear as the most suitable choice for predicting the seismic response of these bridges, linear models are still extensively and effectively used for the system identification of flexible bridges for long-term monitoring of their in-service conditions. Also, a number of vibration based damage detection algorithms are based on modal features extracted from linear models, and have

been extensively tested on a variety of real structures and lab specimens (Spyrakos et al. 1990, Mazurek and De Wolf, 1990, Liang et al. 1997, Haritos and Owen 2004). Based on these studies, it is generally acknowledged that changes in vibration signatures could be poor indicators of structural deterioration, unless the damage is severe and global in nature. Local changes in mode shapes appear instead as more sensitive indicators of damage. Damage identification methods, based on modal strain variation, proved able to Level III damage recognition (detection, localization and severity estimate, as defined in (Rytter, 1993)) in flexural structures (Topole and Stubbs, 1995, Farrar and Jauregui, 1998, Fu and De Wolf 2001, Benzoni et al., 2013, Derkevorkian et al. 2013). Despite the current availability of a variety of damage identification methods, Damage Index (DI) methods appear particularly suitable for SHM of flexible bridge-like structures based on their robustness in both localizing and quantifying the severity of damages, as furthermore confirmed by a recent review (Fan and Qiao, 2011).

In recent years many retrofit solutions have been used to enhance the seismic response of existing infrastructure and the use of Seismic Response Modification Devices (SRMD), such as isolators and energy dissipating devices, is considered one of the most cost effective innovative strategy for critical infrastructure. Friction-based isolators, lead-rubber bearings, and viscous dampers are, among others, technical solutions extensively used to enhance the performance of critical infrastructure in case of seismic events. Remarkable examples of these applications, presented in this work as case studies, are the Vincent Thomas Bridge, the Benicia Martinez Bridge and the Yokohama Bay Bridge. It is however well accepted that any deficiency in the

\* University of California San Diego, Department of Structural Engineering, La Jolla, Ca, USA

\*\* California State Polytechnic University, Department of Civil Engineering, Pomona, Ca, USA

Corresponding Author: Gianmario Benzoni - benzoni@ucsd.edu

expected behavior of these devices can make the structure significant vulnerable to earthquake loads. If the periodic bridge inspection is supported by a validated SHM approach, devices with degraded performance can be early identified before they compromise the performance of the whole structure (Bonessio et al. 2012, Benzoni et al. 2011).

In this study, an overview of a damage detection method (Level III) is presented with examples for numerical and experimental validation.

## 2. Damage detection algorithm

The proposed approach (Bonessio et al. 2012) uses acceleration records from a dispersed set of sensors to obtain information about the condition of the entire structure. The core of the algorithm compares the modal energy of the structure in the undamaged and damaged state, as indicative of the degradation experienced on local portions of the overall structural assembly. A structural identification pre-processing procedure is required in order to evaluate modal characteristics of the structure from the acceleration records.

The application of the procedure requires a sub-division of the skeletal structure into an arbitrary number of elements  $N_E$ . A damage localization ratios  $\beta_{i,jk}$  is calculated for all the  $j$ -th elements with respect to an arbitrary chosen  $k$ -th element.

$$\beta_{i,jk} = \frac{\int_{L_j} \varepsilon^*{}^2 dl}{\int_{L_j} \varepsilon^2 dl} \cdot \frac{\int_{L_k} \varepsilon^2 dl}{\int_{L_k} \varepsilon^*{}^2 dl} \quad (1)$$

where  $\varepsilon$  and  $\varepsilon^*$  are the predominant strain terms for the  $j$ -th element in the undamaged and damage condition, respectively. The predominant strain terms are calculated from the mode shape of each mode  $i$ .  $L$  is the length of each sub-element of the arbitrary discretization of the structural components (deck, piers, etc.). The damage localization ratios  $\beta_{i,jk}$  can be normalized to the minimum of the ratios calculated for each  $j$ -th element with respect to the reference  $k$ -th element ( $\beta_{i,k_{\min}}$ ):

$$\beta_{i,j} = \frac{\beta_{i,jk}}{\beta_{i,k_{\min}}} \quad (2)$$

The localization terms  $\beta_{i,j}$  for the  $j$ -th element can be computed for different mode shapes and combined in a multi-modal term:

$$\beta_j = \sum_{i=1}^n \gamma_i \beta_{i,j} \quad (3)$$

where  $n$  is the number of considered modal shapes and  $\gamma_i$  a reliability parameter for each modal contribution defined as:

$$\gamma_i = \frac{(1/q_i)^a}{\sum_{i=1}^n (1/q_i)^a} \quad (4)$$

with

$$q_i = \frac{\sum_{j=1}^{N_E} (\beta_{i,j} - 1)}{N_E} \quad (5)$$

where  $N_E$  is the number of elements and is an exponent based on engineering judgment. For values  $a \gg 1$  the reliability criterion becomes extremely selective and only the mode with the lower value of  $q_i$  is considered reliable in the assessment of  $\beta_{i,j}$ . In general higher values of  $a$  are suggested in case of limited availability of sensors and thus questionable dependability of higher mode shapes. A value of  $a = 2$  proved to be effective for the case studies taken into consideration. The term  $q_i$  is the average of the deviation of the normalized terms  $\beta_{i,j}$  from the value 1 (i.e. from the hypothetical condition of no damage).

The damage occurrence is given by the 98% probability condition when:

$$Z_j = \left| \frac{\beta_j - \bar{\beta}}{\sigma_{\beta}} \right| \geq 2 \quad (6)$$

where the parameters  $\bar{\beta}$  and  $\sigma_{\beta}$  represent the mean and the standard deviation of  $\beta_j$ , respectively. A damage severity index is obtained, for each  $j$ -th element, as:

$$\alpha_j = (\beta_j)^{-0.5} - 1 \quad \alpha_j \geq -1 \quad (7)$$

This index corresponds to the fractional change in stiffness for traditional structural elements such as beams or piers while for elements such as isolators and energy dissipators it needs to be interpreted in terms of a device-specific performance parameter.

## 3. Physical interpretation of damage index

For the bridge structures of this study two types of anti-seismic devices were considered. The first type belongs to the family of curved friction-based isolators characterized by the following force-displacement relationship (Almazan et al., 1998):

$$F_b = U_b \frac{W}{R} + \mu W \operatorname{sgn}(\dot{U}_b) \quad (8)$$

where  $F_b$  is the shear force across the isolator,  $U_b$  is the bearing displacement,  $\dot{U}_b$  is the sliding velocity across the bearing,  $W$  is the supported weight,  $R$  is the radius of curvature of the bearing concave surface and  $\mu$  is the coefficient of friction mobilized during sliding.

The second category of devices consists of energy dissipators, e.g. viscous dampers, commonly modeled by the following equation:

$$F_d = c |\dot{U}_d|^N \operatorname{sgn}(\dot{U}_d) \quad (9)$$

where  $F_d$  is the axial force of the damper,  $\dot{U}_d$  is the velocity of the relative motion between the two ends of the damper,  $c$  is the viscous coefficient,  $N$  is a real

positive exponent with typical values in the range of 0.1 to 1. Due to the non-linear behavior of the friction isolators and the velocity-dependent behavior of the viscous dampers, modifications of their stiffness, identified through the  $\alpha$  index, can be detected when device performance characteristics changed as well as when changes of the relative displacement across the isolator and/or of the relative velocity across the dampers are experienced. Relative displacement variations, for instance, cause values  $\alpha_i \neq 0$  also in undamaged devices introducing false-positive damage detection. As an example, a damaged condition affecting one isolator can involve a reduction of the relative displacement for all the isolators. This reduction corresponds to an apparent stiffness increment and a consequent higher value of  $\alpha$  in all the isolators including the undamaged ones.

For this reason, in order to interpret the significance of the  $\alpha_j$  values for the anti-seismic devices and to isolate the real occurrence of damage, an additional level of information was required and was provided as fractional change in the relative displacements  $\delta_j$  across the devices, introduced as:

$$\delta_j = \frac{\Delta\sigma_j}{\sigma_j} = \frac{\sigma_j^* - \sigma_j}{\sigma_j} \quad (10)$$

being  $\sigma_j$  and  $\sigma_j^*$  the standard deviation of the relative displacement between the top and the bottom of the isolators, measured in the undamaged condition and in the damaged condition, respectively. With this additional information, given the response of the friction-based devices of Eq. 8, the damage severity index can be converted in an indicator of the fractional variation of the friction coefficient, obtained as:

$$\frac{\Delta\mu_j}{\mu_j} = (1 + \delta_j) \left[ \alpha_j \left( \frac{\sigma_j}{\mu_j R_j} + 1 \right) + 1 \right] - 1 \quad (11)$$

where  $R_j$  is the radius of the sliding surface, and  $\mu_j$  is the original friction coefficient of the devices. In a similar manner, expressing the energy dissipated by viscous dampers with  $N = 1$  in Equation (9), the fractional variation  $\Delta\xi_j/\xi_j$  of their damping ratio is obtained as:

$$\frac{\Delta\xi_j}{\xi_j} = \alpha_j \frac{\dot{\sigma}_j \sigma_j^*}{\sigma_j \dot{\sigma}_j^*} - 1 \quad (12)$$

being  $\sigma_j$ ,  $\sigma_j^*$  and the  $\dot{\sigma}_j$ ,  $\dot{\sigma}_j^*$  the standard deviation of the relative displacement and velocity across the dampers measured in the undamaged and damaged condition, respectively.

#### 4. Numerical validation

As mentioned above, the proposed approach can be activated by the availability of accelerometric records from a basic sensor network typically available for bridge structure. The algorithm does not require, for its implementation, a Finite Element model of the struc-

ture. However, for the numerical validation of this procedure non-linear models were implemented in ADINA in order to obtain response records for the undamaged configuration and for simulated damaged conditions.

Two structural systems were considered, representing the Vincent Thomas Bridge and a portion of the Benicia Martinez equipped with viscous dampers and friction isolators, respectively. The structures have been subjected to a white noise in the frequency range of 0.05-10Hz, with components both in vertical and horizontal directions. From the response obtained via numerical simulation the mode shapes were assessed through the use of the Covariance Driven Stochastic Subspace Identification Method by Peeters (Peeters, 2000).

##### 4.1. Vincent Thomas Bridge Model

The Vincent Thomas Bridge is of a cable-suspension bridge 766 m long, with a main suspended span of approximately 457.2 m, two suspended side spans of 154.4 m each, a roadway width of approximately 15.8 m. The bridge is equipped with four sets of dampers located between towers and spans, as indicated in the detail of Figure 1.

For a numerical simulation of damage, 8 cases were investigated as reported in Table 1. Each scenario represents a simulated damage event, localized in the viscous dampers and in one element of the bridge superstructure. The damage in the superstructure was introduced by reducing the elastic modulus of the appropriate elements, while the degradation of the damper performance was modeled as a reduction of its damping ratio. In case #1, #2 and #3 the damage has been introduced in the damper D1 (East span to East tower) with different levels of intensity (high, medium and low).

It must be noted that the predicted stiffness variation appears spread between both the dampers converging on the same tower (D1 and D2). The two sets of damper, in fact, work as a parallel system in connecting the deck to the tower. The same consideration applies to the couple of dampers D3-D4. In the damage detection algorithm only in-plane vibrational modes have been used, with the longitudinal swinging mode of the bridge as principal contributing component. To distinguish damages in dampers concurring to the same tower, lateral modes should be included in the analysis and 3D deformations of the structure have to be considered. The severity index values of Table 1 was calculated as in Equation (7). Stiffness variations have been translated into variations of damping ratio by Eq. 12 and reported in the last column of Table 1. The localization terms  $\beta_j$ , obtained from a multimodal analysis are combined (Eq. 3) using the first three modes of the structure and are graphically reported in Fig. 2 for each element of the case study #6. The index  $Z_j$  shows a clear localization of the damage in element D3, D4 and 17. The damage severity index of Table 1 shows a good agreement with the simulated damage level. It also indicates, when compared with the predicted variation of damping ratio, that the se-

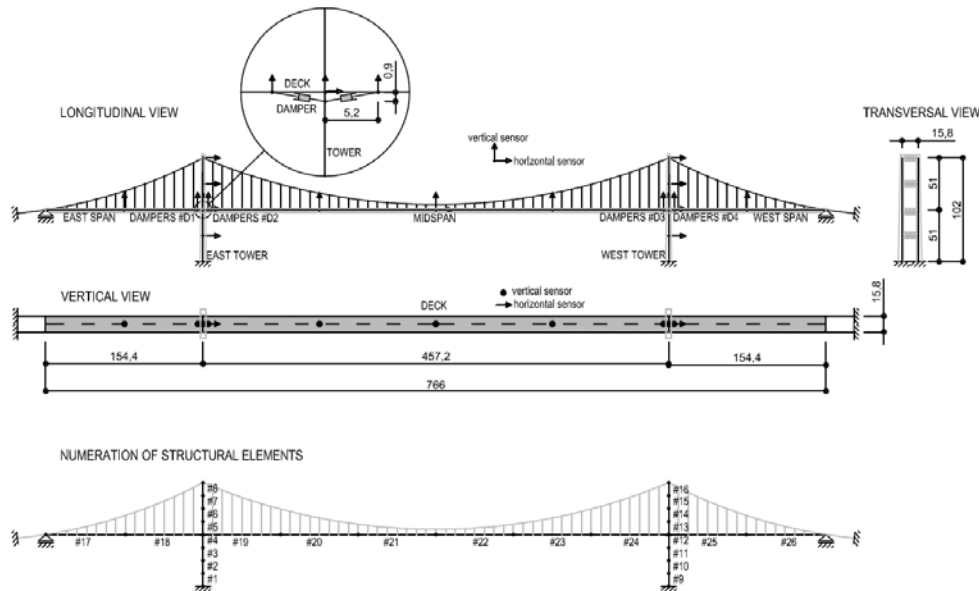


Fig. 1. Layout of the Vincent Thomas Bridge with viscous dampers. The numeration of structural elements used for the algorithm is showed. Configurazione del ponte Vincent Thomas con smorzatori viscosi (dampers). È riportata la numerazione degli elementi utilizzata nell'implementazione dell'algoritmo.

Tab. 1. Simulated damages and predicted stiffness variations for bridge with viscous dampers. Danni simulati e variazioni di rigidezza identificate per il ponte con smorzatori viscosi.

Damage case	Simulated damage		Predicted Stiffness Variation		Predicted Variation of damping ratio. $\Delta\xi_y/\xi_y$ (Eq. 12)
	Location	Severity <sup>+</sup>	Location	Severity <sup>+</sup> $\alpha$ (%)	
1	D1	-50	D1, D2	-25.6, -25.3	-25.4, -25.1
2	D1	-25	D1, D2	-11.8, -11.6	-12.2, -12.0
3	D1	-10	D1, D2	-5.4, -5.6	-5.2, -5.3
4	D1, D2	-25, -25	D1, D2	-25.2, -25.2	-25.2, -25.2
5	D1, D2, D3, D4	-25, -25, -25, -25	D1, D2, D3, D4	-24.9, -25.3, -25.3, -24.9	-24.9, -25.3, -25.3, -24.9
6	D3, D4, 17	-25, -25, -25	D3, D4, 17	-25.01, -25.04, -25.6	-25.01, -25.04, N/A
7	17	-50	17	-48.4	N/A
8	17	-25	17	-25.03	N/A

<sup>+</sup>Severity (%) =  $(E^* - E)/E \times 100$  for column elements.  
=  $(\mu^* - \mu)/\mu \times 100$  for viscous dampers.

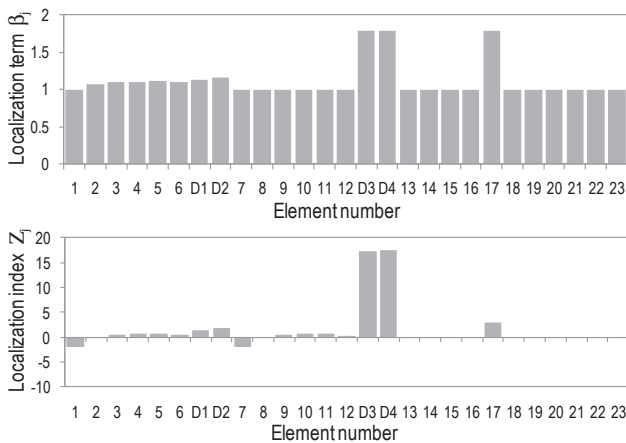


Fig. 2. Localization term  $\beta_j$  and index  $Z_j$  for damage case #6. Coefficienti di localizzazione  $\beta_j$  e indice  $Z_j$  per il caso #6.

verity index, for this type of devices, can be directly interpreted as variation of damping capacity with an acceptable level of accuracy.

#### 4.2. Benicia Martinez Bridge Model

This bridge structure offers, in contrast with the previous example, the possibility to analyze a scenario where the direct interpretation of the severity index is not feasible due to the nature of the installed anti-seismic devices. The Benicia-Martinez bridge is, in fact, equipped with friction-based isolators (FP), installed at the top of the piers between deck structure and cap beams. (Figure 4). This configuration introduces an additional level of complexity in the physical interpretation of the severity that can be directly interpreted as severity of the simulated damage only for the deck and pier elements. As mentioned above, due to the non-linear behavior of the friction-based isolators, increments of their stiffness can be related to either increments of the frictional characteristics or to the reduction of the relative displacement experienced across the isolator. For this reason it is a paramount importance to discern when a stiffness variation, identified by the monitoring procedure, corresponds to a real degradation of the device performance.

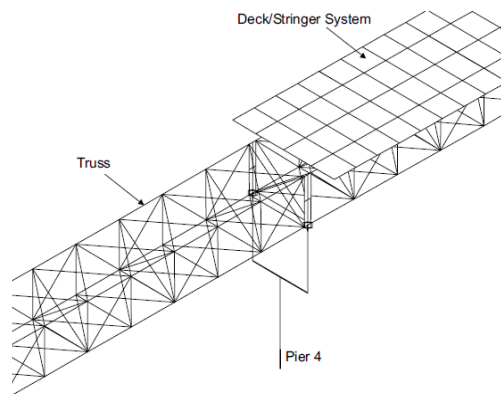


Fig. 3. Close-up Isometric View of ADINA Model of the Benicia Martinez Bridge. Particolare del modello ADINA della struttura del ponte Benicia Martinez.

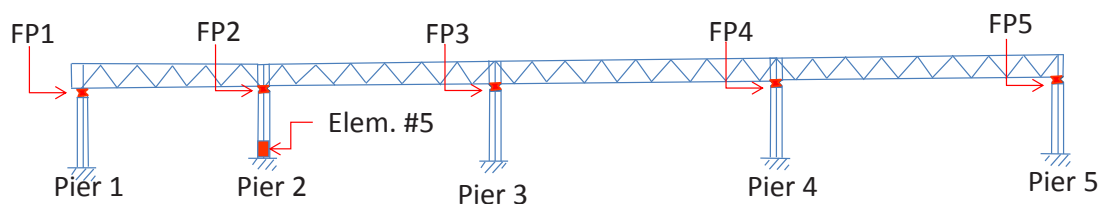


Fig. 4. Layout of the bridge with friction isolators. Schema del ponte con isolatori ad attrito (FP).

Tab. 2. Simulated damages and predicted variations on friction-based isolators. Danni simulati e variazioni stimate delle caratteristiche degli isolatori attritivi.

Damage case	Simulated damage		Predicted Stiffness Variation		Variation of friction coeff
	Location	Severity <sup>+</sup>	Location	Severity index $\alpha$ (%)	
1	FP2	+50	FP1, FP2, FP3, FP4, FP5	(+6.9), +30.4, (+7.1), (+7.1), (+6.9)	(+0.0), +50.6, (+0.5), (+0.5), (+0.5)
2	FP2	+25	FP1, FP2, FP3, FP4, FP5	(+6.1), +17.7, (+6.2), (+6.2), (+6.1)	(+0.0), +25.4, (+0.4), (+0.4), (+0.0)
3	FP2	+10	FP1, FP2, FP3, FP4, FP5	(+5.6), +11.0, (+5.7), (+5.8), (+5.6)	(+0.0), +12.1, (+0.5), (+0.4), (+0.0)
4	FP2, FP5	+25,+25	FP1, FP2, FP3, FP4, FP5	(+6.4), +18.2, (+6.6), (+6.6), +17.9	(+0.0), +25.5, (+0.5), (+0.5), +25.0
5	5	-50	5, FP1, FP2, FP3, FP4, FP5	-50.0, (+5.5), (+5.6), (+5.6), (+5.6), (+5.5)	N/A, (+0.0), (+0.4), (+0.3), (+0.2), (+0.0)
6	5	-10	5, FP1, FP2, FP3, FP4, FP5	-9.9, (+5.5), (+5.6), (+5.6), (+5.6), (+5.5)	NA, (+0.0), (+0.3), (+0.3), (+0.2), (+0.0)
7	5, FP2	-10, +25	5, FP1, FP2, FP3, FP4, FP5	-9.9, (+5.9), +17.5, (+6.0), (+6.1), (+5.9)	NA, (+0.9), +26.8, (+1.2), (+1.2), (+0.9)

<sup>+</sup>Severity (%) =  $(E^* - E)/E \times 100$  for column elements.  
 $(\mu^* - \mu)/\mu \times 100$  for FP isolators.

The Finite Element model of a segment of the bridge (Fig. 4) was subjected to a white noise (0.05-10Hz), in both vertical and horizontal direction. Degradation of the isolator performance was, for this case study, modeled as an increase of the friction coefficient  $\mu$ , while degradation of the piers and the superstructure was simulated by reducing the elastic modulus of appropriate elements (i.e. reducing the stiffness). Several damage cases were investigated. Seven cases are reported in Table 2 in terms of simulated damage location and severity. The predicted stiffness variation shows the locations where a damage is assessed and the severity of the damage ( $\alpha$ ) based on the contribution of three fundamental modes. The values of  $\alpha$  reported in parentheses are false damage conditions identified by the procedure for the above mentioned reasons. However, the availability of the relative displacement and

the use of Eq. 10 allows, during the physical interpretation of the damage severity index, to remove almost completely the false assessment, as indicated in the last column of Table 2.

## 5. Experimental data

### 5.1. Vincent Thomas Bridge – in field data

The limited sensor network currently installed on the Vincent Thomas bridge allowed the acquisition of ambient-vibration acceleration records, collected from 2003 to 2011. A total of 13 sets (Table 3) have been used in order to validate the proposed SHM algorithm against realistic data. Data recorded in December 2006 represent a reference (undamaged) due to the pristine

Tab. 3. *Acceleration data set.*  
Set di dati accelerometrici.

No	Year	Date	Hour	Record Length (s)
1	2003	Apr	–	380.0
2	2006	June	–	129.0
3	2006	7 Dec	14:57:40.0	67.0
4	2007	11 July	08:58:27.0	58.0
5	2007	7 August	09:31:37.0	61.0
6	2011	7 June	09:59:38.0	54.0
7	2011	7 June	21:59:39.0	55.0
8	2011	14 June	09:59:38.0	54.0
9	2011	14 June	21:59:39.0	54.0
10	2011	21 June	09:59:38.0	54.0
11	2011	21 June	21:59:39.0	54.0
12	2011	28 June	09:59:38.0	54.0
13	2011	28 June	21:59:39.0	54.0

Tab. 4. *Modal frequencies (Hz).*  
Frequenze modali (Hz).

Event #	1 <sup>st</sup> mode	2 <sup>nd</sup> mode	3 <sup>rd</sup> mode	4 <sup>th</sup> mode
1	0.225	0.399	0.432	0.580
2	0.225	0.361	0.440	0.580
3	0.234	0.360	0.457	0.567
4	0.235	0.346	0.440	0.553
5	0.227	0.366	0.440	0.580
6	0.240	0.350	0.440	0.547
7	0.240	0.350	0.466	0.547
8	0.240	0.346	0.432	0.553
9	0.240	0.350	0.432	0.580
10	0.240	0.372	0.433	0.553
11	0.220	0.350	0.432	0.553
12	0.220	0.346	0.432	0.580
13	0.224	0.346	0.440	0.580

conditions of the dampers after a replacement intervention.

The vertical component of motion of the deck was used for the damage detection procedure applied to the deck structure between mid-span and the East tower (Fig. 1). The motion in the bridge's longitudinal direction was analyzed in order to detect possible degradation in the elements of the East Tower. The vertical motion of the deck and the motion in longitudinal direction were used to estimate possible degradation in the dampers between main span and East tower and between East side span and East tower. Modal characteristics of the first four vertical modes were identified from each of the acceleration data sets of Table 3 and reported in Table 4.

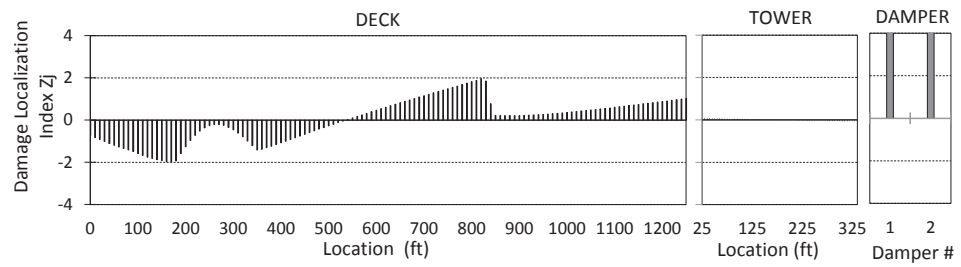
In agreement with the observations of Cross et al. (2011), higher modes frequencies were found more subjected to changes than the 1<sup>st</sup> mode. A maximum variation (0.05Hz) was found for the 2<sup>nd</sup> (asymmetric mode) vibration frequency, while the 1<sup>st</sup> (symmetric mode) frequency is more stable, with a variation of about 0.02 Hz through the whole range of events. The damage identification procedure combined the results of four modes through Eq. 3 indicating a larger contribution to the multimodal damage indices from the first and second mode.

The analyses indicated no damage in the deck and in the towers for events #1 and #2, occurred before

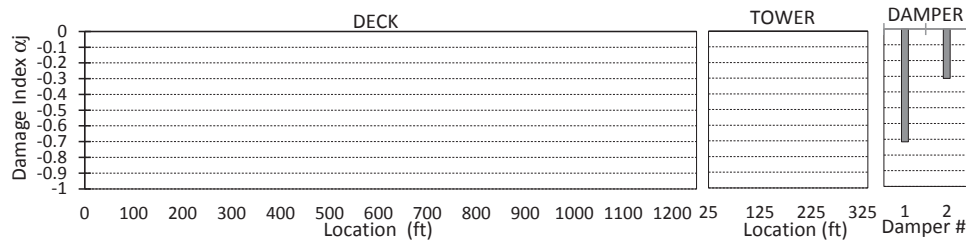
December 2006 and so before the dampers' replacement. For the dampers connecting the tower to the main span, instead, a consistent reduction of stiffness was detected. The amount of the effective stiffness reduction was higher than 80%, indicative of a severe reduction of the dissipative performance of the dampers. The devices indicated by the SHM procedure as potentially damaged were removed from the bridge, replaced with new devices, and tested at the Caltrans SRMD Testing Facility in San Diego, confirming critical conditions. For the events after Decembers 2006, i.e. events #4 to #13, no significant stiffness reduction was identified for the tower. In events #6, #8, and #12 (Fig. 5), negligible stiffness reductions were localized in the portion of the deck close to the tower, where the dampers are connected. For the viscous dampers however, when comparing the responses of 2007 and 2011 with the undamaged scenario of 2006, severity index values of -13% and -58% were identified.

## 5.2. Yokohama Bay Bridge –in field data

Opened September 27, 1989, the Yokohama Bay bridge (YBB) crosses the Tokyo Bay with a 3-span continuous deck plate (main span of 460 m) and is part of the Bayshore Route of the Shuto Expressway. The



a)

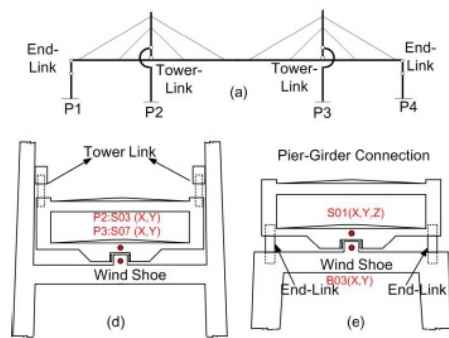


b)

Fig. 5. Damage localization indicator and damage severity index – 2011, Jun 28 - 10PM (#12).  
Indicatore della localizzazione del danno ed indice di severità - 2011, Giugno 28 - 10PM (#12).



Fig. 6. Yokohama Bay Bridge (source: www.yokogawa-bridge.co.jp/).  
Ponte Yokohama Bay (www.yokogawa-bridge.co.jp/).



Tab. 5. Acceleration data sets.  
Set di dati accelerometrici.

Event name	Trigger time (JST)	Length (s)	Mw	Distance (mi) [km]
MS (main shock)	2011/03/11 14:47:45.00	600.00	9.0	247 [398]
AS #1	2011/03/11 15:16:16.00	480.00	7.7	119 [192]
AS #2	2011/03/11 15:27:20.00	240.00	7.5	352 [567]
AS #3	2011/03/11 16:29:33.00	60.00	6.5	375 [603]
AS #4	2011/03/11 17:20:14.00	180.00	6.1	183 [295]
AS #5	2011/03/12 04:00:21.00	120.00	6.7	127 [205]
AS #6	2011/03/13 10:27:11.00	120.00	6.4	144 [233]
AS #7	2011/03/14 10:03:33.00	60.00	6.2	126 [204]
AS #8	2011/03/15 22:32:08.00	120.00	6.4	40 [64]
AS #9	2011/03/16 12:52:41.00	120.00	6.1	92 [148]

main girder consists of a double-deck steel truss-box with six lanes upper deck and two lanes lower deck. The bridge has two H-shaped towers welded as monolithic section with the height of 172m and width of 29.25m (Figure 6). The girder is suspended from tow-

ers and end piers by means of link-bearing connections aimed at reducing effects of the superstructure inertia forces on the substructure in case of an earthquake, while maintaining a longitudinal fundamental period of about 7.7 sec (Siringorino and Fujino, 2012). The

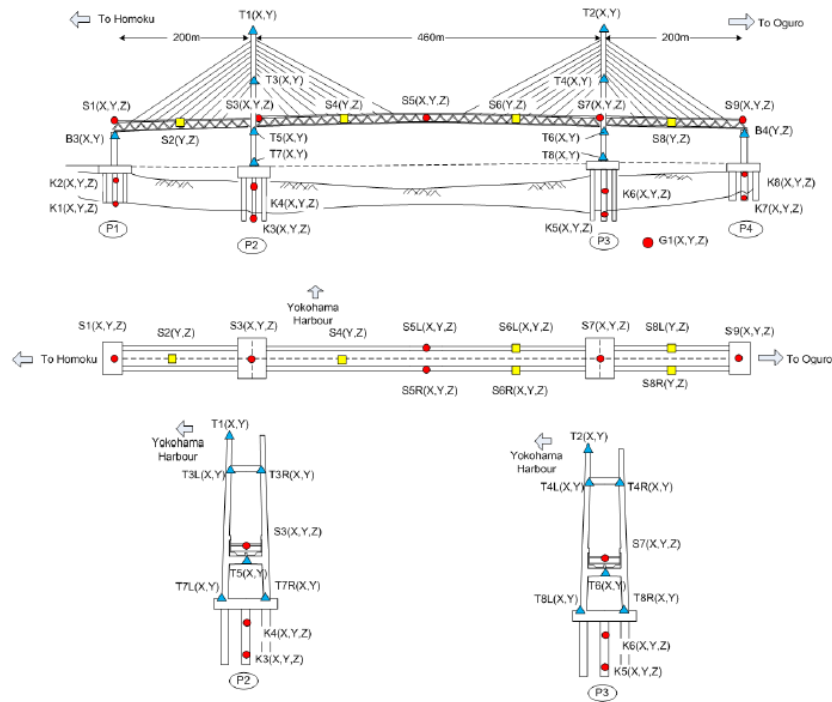


Fig. 7. Sensor network on the Yokohama Bay Bridge: squares = bi-directional accelerometers in lateral (Y) and vertical (Z) direction, triangles = bi-directional accelerometers in longitudinal (X) and vertical (Z) direction, circles = tri-directional accelerometers (X, Y, Z).  
 Rete di sensori del ponte Yokohama Bay: quadrati=accelerometri bidirezionali in direzione laterale (Y) e verticale (Z), triangoli =accelerometri bidirezionali in direzione longitudinale (X) e verticale (Z), cerchi = accelerometri tri-direzionali (X, Y, Z).

Tab. 6. Statistics of the identified vibration frequencies of the YBB fundamental modes  
 Valori statistici delle frequenze identificate per i principali modi del ponte YBB.

Mode	Frequency (Hz)	
	Average±sd	COV
1st Longitudinal	0.118 ± 0.017	0.144
1st Lateral	0.295 ± 0.011	0.037
1st Vertical	0.372 ± 0.022	0.059

link-bearing connection consists of a double-head steel pendulum (10 m and 2 m long for end-links and tower-links, respectively) and steel-PTFE sliding bearings. In transverse direction, the girder movement is restricted by wind shoes at all piers and towers. Transverse gaps exist between wind shoe and girder to allow for tower-girder transverse relative motion.

The YBB experienced the 2011 Tohoku earthquake sequence, an undersea megathrust ground shaking event with a main shock of magnitude 9.0 (Mw) that occurred on the March 11th 2011. A total of 10 sets of acceleration histories (Table 5) during the main shock and aftershock events between March 11th and 15th were recorded by a network of 36 accelerometers installed onto the bridge as shown in Figure 7. This extensive set of acceleration data was used to identify modal characteristics and possible damages on the bridge.

The algorithm was applied to the bridge to detect damages with respect to a reference (undamaged) condition obtained from the first 20 seconds of the main shock acceleration data. Main dynamic characteristics are reported in Table 6. The damage localization in-

dex  $Z_j$  and the damage severity index  $\alpha_j$  are plotted in Figure 8 for the deck, the devices (connection links) and the piers after the main shock. The results for the two piers are consecutively plotted on the same graph. Damages on the deck are identified when the  $Z_j$  index exceeds the value +2. It is visible from Figure 8 that two occurrences slightly exceed the damage threshold. However, they appear as false positives numerically generated by close-to-zero values of the curvature of the deck in the vertical mode. In case of very small curvature values, in fact, even a small variation between the reference and the present condition corresponds to a high increment of the  $Z_j$  index. Using many vibration modes in vertical direction would reduce the occurrence of this type of false-positives. It should also be noticed that the peak values of the  $Z_j$  index correspond to very limited damage severity ( $|\alpha_j| < 5\%$ ).

The degradation in the connection links is identified by the values of that significantly exceed the threshold of 2. The severity  $\alpha_j$  associated with this occurrence is about -0.6, indicating a 60% reduction of stiffness occurred during the main shock. This reduction of stiffness could be attributed to transition between a predominantly stick behavior of the bearing-link connections to a predominantly slip behavior. From the visual inspection reported in (Siringorino and Fujino 2012), scratches were found on the wind shoes of the tower #2 suggesting that the girder had experienced large relative longitudinal movement. For this relative displacement to occur, the link-bearing connections between girder and tower must have slipped. Even for the low intensity after shock #3, a similar distribution of damages along the structure was identified. In summary, based on the

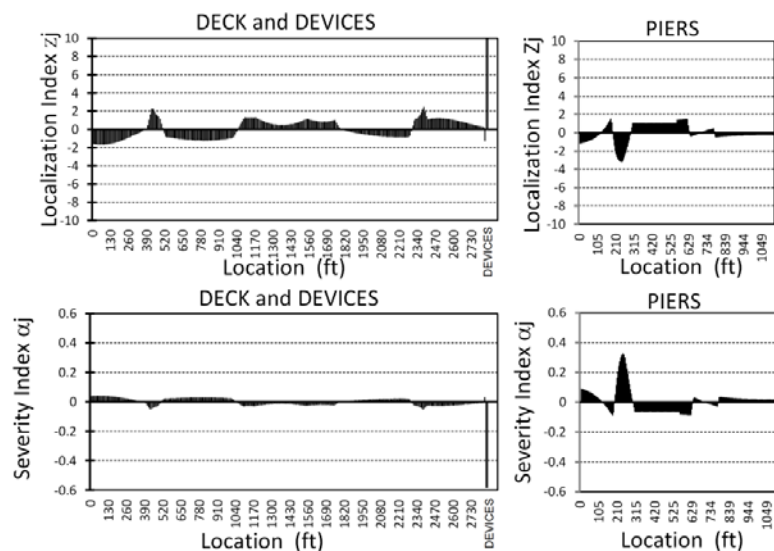


Fig. 8. Damage index for the main shock.  
Indice di danno per l'evento principale.

results of the damage detection procedure, no structural damage to the Yokohama Bay Bridge was identified for the main shock excitations and the following after-shocks. This is in agreement with the design expectations, since the excitations were considerably below the design and seismic-retrofit seismic loads (Maeda et al. 1991). The identified changes in stiffness for the link-bearing connections are most likely associated with the nonlinear frictional behavior of the link mechanism.

## 6. Conclusions

The most distinctive aspects of the adopted Damage Identification method are: (1) its capability of detecting damages in traditional structural members, as well as in seismic devices, which are included at the design stage or for retrofit purposes in a number of modern suspension and cable-stayed bridges; (2) its high level of automation, which made it suitable for implementation in an executable software for SHM of bridge structures (Benzoni et al., 2011); (3) the possibility of implementing a multi-mode combination of localization terms which allows without any pre-screening/post-selection of either the direction of vibration or of the mode shapes; (4) the possibility to link the damage severity index to the devices' fundamental performance parameters.

## References

- Almazan J.L., De la Llera J.C. and Inaudi, J.A. [1998]. "Modeling aspects of structures isolated with the friction pendulum system". *Earthquake Engineering and Structural Dynamics* 27: 845-867.
- Aktan, A.E., Catbas, F.N., Grimmelsman, K.A. and Tsikos, C.J. [2000]. "Issues in infrastructure health monitoring for management", *Journal of Engineering Mechanics*, ASCE 126: 711-724.
- Benzoni, G., Bonessio, N. and Lomiento, G. [2011]. "Structural Health Monitoring of Bridges with Anti-Seismic Devices", Proceedings of the 8th European Conference on Structural Dynamics. Eurodyn, Leuven, Belgium 4-6 July.
- Benzoni, G., Bonessio, N. and Lomiento, G. [2013]. "Structural health Monitoring of Bridges with Seismic Response Modification Devices", Report no. SSRP-13/02. Department of Structural Engineering UCSD, May, San Diego.
- Bonessio, N., Lomiento, G. and Benzoni, G. [2012]. "Damage identification procedure for seismically isolated bridges", *Structural Control and Health Monitoring* 19(5): 565-578.
- Carden, E.P. and Fanning, P. [2004]. "Vibration based condition monitoring: a review", *Structural Health Monitoring* 3(4): 355-377.
- Cross, E., Worden, K., Koo, K.Y. and Brownjohn, J.M. [2011]. "Modelling environmental effects on the dynamic characteristics of the Tamar suspension bridge", *Dynamics of Bridges*, Volume 5 (pp. 21-32). Springer, New York.
- Derkevorkian, A., Masri, S.F., Benzoni, G., Lomiento, G. and Bonessio, N. [2013]. "Evaluation of the Efficacy of Some Promising Algorithms for Damage Detection, Location, and Quantification in Seismic Response Modification Devices and Flexible Bridges", California Department of Transportation Technical Report November.
- Fan, W. and Qiao, P. Z. [2011]. "Vibration-based damage identification methods: a review and comparative study", *Structural Health Monitoring* 10(5), 83-111.
- Farrar, C.R. and Jauregui, D.A. [1998]. "Comparative study of damage identification algorithms applied to a bridge: I. Experiment", *Smart Materials and Structures* 7(5): 704-719.
- Frangopol, D. and Liu, M. [2007]. "Maintenance and management of civil infrastructure based on con-

- dition, safety, optimization, and life-cycle cost”, *Structure and Infrastructure Engineering*, 10.1080/15732470500253164; 29-41.
- Fu, Y. and De Wolf, J.T. [2001]. “Monitoring and analysis of a bridge with partially restrained bearings”, *Journal of Bridge Engineering* 6(1): 23-29.
- Haritos, N. and Owen, J.S. [2004]. “The use of vibration data for damage detection in bridges: a comparison of system identification and pattern recognition approaches”, *Structural Health Monitoring* 3(2): 141-163.
- Liang, Z., Lee, G.C. and Kong, F. [1997] “On detection of damage location of bridges”, Proceedings of SPIE, the International Society for Optical Engineering 3089: 308-312.
- Lus, H., Betti, R. and Longman, R.W. [1999]. “Identification of linear structural systems using earthquake-induced vibration data”, *Earthquake Engineering and Structural Dynamics* 28(11): 1449-1468.
- Maeda, K., Otsuka, A. and Takano, H. [1991]. “The design and construction of Yokohama Bay Bridge, Cable-Stayed Bridges Recent Developments and their Futures”. M. Ito et al. (Editors). Elsevier Science Publisher B.V., 377-395.
- Mazurek, D.F. and De Wolf, J.T. [1990]. “Experimental study of bridge monitoring technique”, *Journal of Structural Engineering* 116 (9): 2532-2549.
- Okasha, N., Frangopol, D. and Orcesi, A. [2012]. “Automated finite element updating using strain data for the lifetime reliability assessment of bridges”, *Reliability Engineering & System Safety*, 10.1016/j.res.2011.11.007; 139-150.
- Peeters, B. [2000]. “System Identification and damage detection in civil engineering”, Ph.D. thesis Department of Civil Engineering. K.U. Leuven, Belgium.
- Rytter, A. [1993]. “Vibrational based inspection of civil engineering structure”, PhD dissertation, University of Aalborg, Denmark.
- Siringorino, D.M. and Fujino, Y., [2012]. “Response Analysis of Yokohama Bay Bridge under the 2011 Great East Japan Earthquake”, Proc. 15th World Conference of Earthquake Engineering, Lisbon, Portugal.
- Siringorino, D.M. and Fujino, Y. [2006]. “Observed dynamic performance of the Yokohama-Bay Bridge from system identification using seismic records”, *Structural Control and Health Monitoring* 13(1): 226-244.
- Soyoz, S. and Feng, M.Q. [2009]. “Long-Term Monitoring and Identification of Bridge Structural Parameters”, *Computer Aided Civil and Infrastructure Engineering* 24(2): 82-92.
- Smyth, A.W., Pei, J.S. and Masri, S.F. [2003]. “System identification of the Vincent Thomas suspension bridge using earthquake records”, *Earthquake Engineering and Structural Dynamics* 32(3): 339-367.
- Spyrakos, C., Chen, H.L., Stephens, J. and Govindaraj, V. [1990]. “Evaluating Structural Deterioration Using Dynamic Response Characterization”, Proceedings of The International Workshop on Intelligent Structures Taipei, Taiwan; 137-153.
- Topole, K.G. and Stubbs, N. [1995]. “Non-destructive damage evaluation of a structure from limited modal parameters”, *Earthquake Engineering and Structural Dynamics* 24(11):1427-1436.
- Yun, H., Nayeri, R., Tasbihgoo, F., Wahbeh, M., Cafrey, J., Wolfe, R., Nigbor, R., Masri, S.F., Abdel-Ghaffar, A. and Sheng, L.H. [2008]. “Monitoring the collision of a cargo ship with the Vincent Thomas Bridge”, *Structural Control and Health Monitoring* 15(2): 183-206.

# Validazione numerica e sperimentale di una tecnica di monitoraggio strutturale per infrastrutture

G. Benzoni, N. Bonessio, G. Lomiento

**SOMMARIO** – Viene qui presentato, insieme ad esempi numerici e sperimentali di applicazione e validazione, un metodo di identificazione delle condizioni di degrado di infrastrutture caratterizzate dalla presenza di dispositivi di isolamento sismico e/o di dissipatori di energia. Il metodo, basato sulla disponibilità della risposta accelerometrica della struttura in un numero limitato di posizioni, è stato inizialmente testato attraverso modelli ad Elementi Finiti in grado di simulare l'esistenza di condizioni di degrado sia in componenti strutturali tradizionali (pila, impalcato etc.) sia nei dispositivi antisismici installati. In particolare sono state modellate, in questa fase, due strutture da ponte quali il Vincent Thomas bridge e il Benicia Martinez bridge, dotati rispettivamente di smorzatori viscosi e di isolatori curvi ad attrito. In una fase successiva la procedura è stata applicata a dati registrati su strutture reali durante oscillazioni ambientali (Vincent Thomas bridge) così come durante eventi sismici (Yokohama Bay Bridge). La procedura si rivela adeguata per l'identificazione di condizioni di degrado in elementi strutturali e in dispositivi antisismici. Oltre a consentire la localizzazione di variazioni di rigidità e la stima della loro intensità, l'approccio proposto conduce all'interpretazione dell'indice di severità in termini di fondamentali parametri di funzionamento dei dispositivi installati.

**Parole chiave:** Monitoraggio strutturale, Identificazione multi-modale del danno, Rete di sensori, Infrastrutture, Dispositivi antisismici.

L'approccio proposto originariamente in Bonessio et al. (2012) utilizza registrazioni accelerometriche ottenute attraverso semplici network di sensori installati su strutture da ponte, allo scopo di stimare le attuali condizioni della struttura, sia nelle sue componenti tradizionali (pile, impalcato ecc.), sia per quanto riguarda dispositivi antisismici installati. L'algoritmo di base confronta l'energia modale della struttura nello stato attuale con quella di una condizione definita di riferimento. Le variazioni rilevate vengono interpretate come indicative di una condizione di degrado generata. Un passaggio preliminare richiede l'identificazione delle caratteristiche modali della struttura. Successivamente, l'applicazione della tecnica di identificazione del danno si sviluppa attraverso il calcolo degli indici definiti in Eq. 1-7. In particolare vengono calcolati, per ogni singolo elemento in cui viene fittiziamente suddivisa la struttura (o parte di essa), un indice di localizzazione (Eq. 3) e un indice di severità (Eq. 7). Va notato come l'indice di localizzazione è ottenuto mettendo in conto più contributi modali (Eq. 3). La condizione di danno viene segnalata da un valore di  $Z$  (Eq. 6) maggiore o uguale a 2 (98% di probabilità). La procedura è stata applicata a situazioni di degrado strutturale artificialmente generate attraverso modelli a Elementi Finiti di due strutture da ponte: il Vincent Thomas bridge e il Benicia Martinez bridge. Entrambi i ponti risultano dotati di dispositivi antisismici, della famiglia degli smorzatori viscosi (Vincent Thomas) e degli isolatori attritivi (Benicia Martinez). L'applicazione a queste due tipologie di ponte e di protezione antisismica rivela livelli di complessità diversi per l'applicazione e l'accuratezza della procedura. Nel caso di strutture dotate di smorzatori viscosi, i dispositivi vengono analizzati, alla stregua di ogni altra componente strutturale, e cioè in termini di variazione di rigidità quantificata attraverso l'indice di severità  $\alpha$  in caso di presenza di danno. La Tabella 1 presenta otto casi di simulazione di danno in smorzatori e/o in un segmento dell'impalcato. La posizione e la severità del danno identificate risultano in buon accordo con i valori simulati. Appare inoltre come la variazione di rigidità indicata dall'indice di severità  $\alpha$  possa essere direttamente interpretata come variazione di smorzamento dei dispositivi. Si nota infatti il buon accordo tra i valori di  $\alpha$  e del rapporto di smorzamento (ultima

colonna a destra in Tabella 1). Più complessa risulta invece la condizione della struttura Benicia Martinez. La presenza di isolatori ad attrito installati all'interfaccia tra pile e impalcato (Fig. 4) fa sì che una condizione di danneggiamento effettivamente verificatasi per un dispositivo possa riflettersi (per esempio come riduzione di spostamento relativo tra impalcato e pila) anche in dispositivi non danneggiati. L'algoritmo identifica queste variazioni di rigidità come errate condizioni di danno indicate in parentesi in Tabella 2. In altri termini, la forte natura non-lineare di questi dispositivi fa sì che variazioni di rigidità identificate a livello dei dispositivi possano essere conseguenza di un effettivo degrado delle caratteristiche attrittive ma anche di una riduzione di spostamento relativo dell'isolatore. Allo scopo di distinguere l'effettiva occorrenza di un danneggiamento (per esempio variazione del coefficiente di attrito in un isolatore) è necessaria l'introduzione di una ulteriore misura, in particolare dello spostamento relativo del dispositivo. La disponibilità di questa informazione consente di interpretare l'indice di severità in termini di variazione di attrito attraverso l'Eq. 11. L'ultima colonna a destra di Tabella 2 mostra inoltre come l'applicazione dell'Eq. 11 risolva (riducendoli a zero) gran parte dei valori di severità tra parentesi (falsi positivi).

Due casi sperimentali consentono una ulteriore validazione della procedura. Diversi eventi di vibrazione ambientale sono stati registrati attraverso la rete di sensori del ponte Vincent Thomas prima, durante e dopo un intervento di sostituzione degli smorzatori viscosi. Assumendo la data più vicina al periodo di sostituzione come momento di condizione intatta per i dispositivi (Dicembre 2006), il confronto con registrazioni precedenti e seguenti questa data rivelano variazioni anche significative della capacità dissipativa di alcuni smorzatori. Questa condizione di degrado è stata confermata attraverso prove di laboratorio su dispositivi rimossi dalla struttura.

Una ultima applicazione riguarda il ponte Yokohama Bay interessato dall'evento sismico di Tohoku del Marzo 2011. L'applicazione della procedura ad un esteso numero di registrazioni non ha rilevato alcuna condizione di danno per le parti strutturali con l'unica eccezione di giunti impalcato-pila che rivelano un cambiamento di rigidità probabilmente associato ad un comportamento attrittivo non lineare dei giunti stessi.